

Probabilistic robust control of rotorcraft

J.F. Horn^{a,*}, D.K. Tolani^b, C.M. Lagoa^c, Q. Wang^b, A. Ray^b

^aDepartment of Aerospace Engineering, The Pennsylvania State University, 233 Hammond Building, University Park, PA 16802, USA

^bDepartment of Mechanical Engineering, The Pennsylvania State University, 329 Reber Building, University Park, PA 16802, USA

^cDepartment of Electrical Engineering, The Pennsylvania State University, 111K Electrical Engineering West, University Park, PA 16802, USA

Received 13 August 2003; accepted 12 September 2004

Available online 27 October 2004

Abstract

This paper presents an approach for the design of reliable high-performance control systems for rotorcraft in order to enhance handling qualities and ensure closed-loop stability. The proposed control system has a two-tier hierarchical architecture. The lower-tier controller is designed using a probabilistic robust control approach. By allowing different levels of risk under different flight conditions, the control system can trade off between stability robustness and nominal performance. The upper-tier supervisory controller monitors the system response for anomalous behavior that might lead to instability or loss of performance. The supervisor may then switch between robust controllers with different levels of risk and performance.

© 2004 Elsevier Ltd. All rights reserved.

Keywords: Helicopter control; Probabilistic robustness

1. Introduction

Future generation rotorcraft will need to meet more stringent handling qualities requirements in order to perform difficult tasks such as air combat, target tracking, and operating in degraded visual environments. The introduction of rotorcraft unmanned aerial vehicles (RUAVs) may raise the bar even higher in terms of the achievable agility and precision maneuvering of rotorcraft. As a result, future-generation rotorcraft control systems should provide higher bandwidth, improved attitude quickness, less cross-coupling and better disturbance rejection than those achieved by current operational rotorcraft control systems. Traditionally, the limitations on flight control performance for rotorcraft have been more restrictive than those of high-performance fixed-wing aircraft. The out-of-plane (flapping) and in-plane (lagging) motion of the rotor blades produce a number of additional dynamic modes

that can couple with the rigid body motion of the fuselage and the flight control system. Rotor dynamics can become dynamically coupled with the fuselage dynamics for high feedback gains. The air resonance phenomenon occurs when one of the lagging modes becomes very lightly damped or even unstable due to this coupling, and has been observed on helicopters with high bandwidth control systems (Dryfoos, Kothmann, & Mayo, 1999).

One approach for achieving higher performance from rotorcraft flight control systems is rotor state feedback (Horn, 2002; Takahashi, 1994). This allows full state feedback with good stability margins, but it also requires specialized sensors to measure the motion of the rotor blades. Another alternative is to use dynamic compensators based on an accurate high-order model of the coupled fuselage/rotor dynamics (Ingle & Celi, 1992). This approach tends to result in complex high-order controllers, and there will always be inherent uncertainties due to modeling errors, variations in aircraft properties, and changing operating conditions.

Robust control theory allows the design of control systems based on a simple low-order plant model with

*Corresponding author. Tel.: +1 814 865 6434;
fax: +1 814 865 7092.

E-mail address: joehorn@psu.edu (J.F. Horn).

well-defined uncertainty bounds that account for model simplifications, non-linearity, and variations in operating conditions. Furthermore, approximate low-order plant models are more readily identified from flight test data and result in less complex control designs. A number of simulation studies have investigated robust control methods on rotorcraft using both H_∞ and μ -synthesis techniques (Sahasrabudhe & Celi, 1997). An H_∞ based controller for a helicopter has also been tested in flight (Smerlas et al., 1998).

It is well known that the demands on system stability robustness and desired nominal performance can be contradictory to each other. The deterministic worst-case robust design can result in an unduly conservative controller and thus degrade system nominal performance. Instead of stability guarantee under worst-case uncertainties, recent results in probabilistic robust control indicate that the complexity of the controller can be greatly reduced and/or system performance can be significantly improved by allowing a small risk of instability (Lagoa, 1999; Lagoa, Li, & Sznaier, 2001a). Furthermore, by specifying different levels of risk in different flight regimes, the control design could obtain a trade off between robustness and nominal performance.

Military rotorcraft handling qualities specifications dictate different levels of flight control system performance when performing various mission tasks (Aeronautical Design Standard-33E-PRF, 1999). For example, if the aircraft is in cruise flight, the bandwidth and attitude quickness requirements are relatively low, and a low-risk/low-performance controller would be adequate. On the other hand, when performing aggressive combat tasks or precision maneuvers, it may be desirable to achieve the maximum available performance. A high-risk controller might be used if there is a mechanism to recover, in the event that the controller initiates instability. The upper-tier supervisory controller can govern the acceptable level of risk as well as the desired level of performance. Such a system would need to monitor the response of the vehicle to detect degradation in performance or stability, and also take into account external inputs such as the current mission task and environmental conditions. The upper-tier supervision would be an appropriate application of discrete-event control.

This paper investigates the application of advanced control theory for high bandwidth flight control on a military rotorcraft using a high fidelity non-linear simulation model. A hierarchical control system architecture is proposed. Discrete-event control is used for upper-tier supervision and probabilistic robust control is used as the lower-tier controller. The supervisory control chooses from a bank of robust control designs with different levels of risk and performance. This paper focuses on the lower-tier probabilistic robust controller,

as applied for lateral-directional control of a helicopter operating in the low-speed flight regime. Frequency weighted uncertainty perturbations are derived based on the discrepancy between the nominal low-order linear model and the identified frequency response of the non-linear model for a range of off-design flight conditions. Several different controllers are designed using μ -synthesis. The radius of uncertainty and the performance weighting for each controller are varied to produce a set of controllers with varying levels of risk and performance. The risk associated with each controller is assessed using Monte-Carlo simulations, in which the uncertainty perturbations are modeled using random transfer functions (Lagoa, Sznaier, & Barmish, 2001b). The controllers are then tested using the non-linear simulation model. Preliminary results show that switching between a high-risk/high-performance controller to a low-risk/low-performance controller can recover the aircraft from the onset of instability.

The crux of this paper is that a small well-defined risk of instability is acceptable only if there is an upper-tier supervisory controller that can detect the onset of instability and quench it by switching to a conservative controller. Therefore, for most of the operating regime, a high performance, aggressive controller can be used. This idea can be easily extended to other non-linear complex dynamical systems where high-performance control action is required but a single control formulation cannot work for the entire operating range.

The paper is organized into eight sections including the present section. Section 2 presents the proposed two-tier control architecture. Section 3 describes the plant modeling and system identification. Section 4 presents the equations of motion of the rotorcraft and the augmented plant model used for μ synthesis. Section 5 presents the details of controller design. Section 6 presents a method for generating sets of random transfer functions for use in the Monte-Carlo analysis of the controller's probabilistic robustness. Section 7 discusses some issues for practical implementation of the controllers on aircraft. Section 8 discusses the results of simulation experiments. The paper is summarized and concluded in Section 9 along with recommendations for future research.

2. Control system architecture

This section presents the proposed control system architecture for future-generation rotorcraft. Fig. 1 shows the two-tier architecture of the rotorcraft control system and its components are described below.

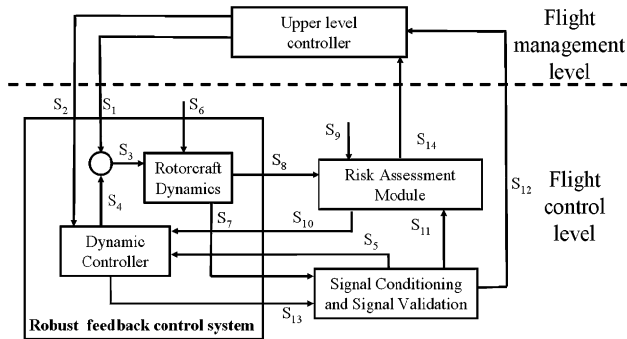


Fig. 1. Rotorcraft control architecture.

2.1. Rotorcraft dynamics

A non-linear dynamic model of the UH-60A Black Hawk helicopter has been adopted for this study (Howlett, 1989). The GENHEL rotorcraft simulation code is widely used by industry and the US government and is accepted as a validated engineering model for handling qualities analysis and flight control design. The code models non-linear aerodynamic effects, and includes fuselage rigid body dynamics, rotor blade flapping and lagging dynamics, rotor inflow dynamics, engine/fuel control dynamics, actuators, and a model of the existing UH-60A automatic flight controls systems (AFCS). The code has been modified to allow for the disengagement of existing AFCS channels and for the integration of the controllers presented in this paper. This subsystem receives the continuous feed-forward control signals S_1 from the upper-tier controller, the exogenous disturbance vector S_6 , and feedback control input vector S_4 from the dynamic controller subsystem. The sensor data vector S_7 , is the output of this subsystem and serves as input to the signal conditioning subsystem. The sensor data set S_8 serves as an input to the risk assessment subsystem.

2.2. Dynamic controller

This subsystem provides the basic inner loop control of the aircraft in order to stabilize the aircraft and satisfy the handling qualities requirements (i.e., performance) over a wide range of operating conditions. In this study, a probabilistic robust controller is designed for a subset of operating conditions. This subsystem receives input signal S_2 from the upper-tier controller, S_{10} from the risk assessment subsystem, and S_5 from the signal conditioning and validation subsystem. This subsystem sends the feedback control vector S_4 to the plant. Given a bound on the risk of instability that is provided by the upper-tier supervisor, the risk-adjusted controller maximizes the nominal performance. In other words, the

controller can trade off between nominal performance and risk of instability.

2.3. Signal conditioning and signal validation

The input this subsystem consists of the sensor signals S_7 (e.g. acceleration, velocity, and angular rate). It also receives information on the linear controller (A, B, C, D matrices) S_{13} . The subsystem provides the processed auxiliary feedback signal S_5 to the dynamic controller. The signal set S_{11} is used by the risk assessment subsystem and the signal set S_{12} is the input to the upper-tier controller.

2.4. Risk assessment subsystem

This subsystem receives input from the signal conditioning subsystem S_{11} , sensor data from the rotorcraft S_8 and external inputs S_9 . Based on these inputs it assesses the risk factor associated with the different controllers using probabilistic methods and sends this information to the robust feedback control system S_{10} and the upper-tier controller S_{14} .

2.5. Upper-tier control

A discrete event supervisor (DES) is used on the flight management level in order to select the controller with the appropriate level of risk and performance for the current flight regime. This subsystem receives the input from the risk assessment subsystem S_{14} and the signal conditioning and validation subsystem S_{12} . The outputs of this subsystem are the reference command signals S_1 and input signals S_2 to the dynamic controller. This paper focuses on the flight control level of the proposed scheme. The development of the upper level controller is part of ongoing research.

3. System identification

Frequency domain identification methods have been shown to be an effective method for identifying accurate linear models of aircraft and particularly rotorcraft. The comprehensive identification from frequency responses (CIFER) analysis tool was developed for this purpose (Tischler, 1991). An advantage of this method is that linear models can be extracted directly from flight data, and the control designer does not rely on theoretical flight dynamics models. Although flight data was not available for this study, a non-linear simulation model is used as a proxy for a real helicopter. The controller is designed using linear models extracted directly from time history data of the non-linear simulation, and then the controllers are tested using this non-linear model. The simulation model generates time histories of the

vehicle response to a sinusoidal input of varying frequency. The frequency response characteristics are identified, and a linear state space model is derived to fit the frequency responses using the CIFER analysis tool. This software uses the chirp-Z transform and composite optimal windowing methods to identify the multi-input–multi-output frequency responses, and a non-linear search algorithm is used to fit a state space model to these frequency responses given a known model structure. Fig. 2 shows the frequency response of the roll rate due to lateral control for the linear model that is identified from the non-linear simulation.

The coherence function is a useful metric to verify that the flight data are satisfactory for system identification. The coherence function γ_{xy} (or partial coherence for a multiple-input–multiple-output system) indicates how well the output y (any of the estimated helicopter states) is linearly correlated with a particular input x over the examined frequency range. It is computed together with the system’s frequency responses, from the cross spectrum G_{xy} , and the input and output auto-spectra G_{xx} and G_{yy} , respectively (note that the partial coherence is derived from the conditioned spectrum); the mathematical definition is

$$\gamma_{xy}^2 = \frac{|G_{xy}|}{G_{xx}G_{yy}} \leq 1. \tag{1}$$

A value of 0.6 is usually used as a lower limit for the coherence function. For lower coherence values, the identified frequency responses will have a large error. In this study, frequency response data with a coherence of 0.8 or higher are used for deriving the plant model.

The linear model of the aircraft is subject to inherent uncertainties. The model is relatively low order (as discussed in the following section) and it matches the full-order dynamics over a very limited frequency range.

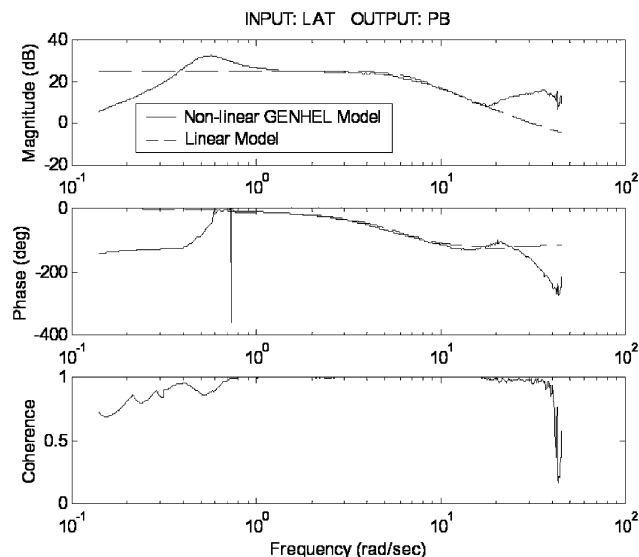


Fig. 2. Roll axis frequency response.

Furthermore, the controller is designed for the low-speed flight regime. It is not normally possible to obtain accurate airspeed measurements below 20 knots (10.292 m/s) on a helicopter, and therefore it is not possible to schedule the controllers with airspeed in this regime. Instead, the controller is designed based on a single nominal linear model for hover, and the controller must be robust to perturbations in the model as the operating point changes within the low-speed envelope. To estimate the uncertainty bounds associated with varying operating conditions, the frequency response characteristics for five flight conditions were calculated: hovering, 20 knots forward, 20 knots right sideward, 20 knots rearward, and 20 knots left sideward flight. Uncertainty bounds are estimated based on the maximum difference between the nominal linear model and the five sets of frequency response data. This is illustrated in Fig. 3, which shows the multiplicative error in each case. The uncertainty weighting functions, $W_{\Delta}(s)$, are designed to cover all operating conditions.

4. The plant model

A reduced order plant model used for design of the lateral-directional controller for hover and low-speed flight is discussed below. The controller is designed to achieve a rate response type in the roll and yaw axes. A simple linear model is optimized to represent the roll and yaw rate dynamics in the frequency range of 1–10 rad/s. The state variables are roll rate, yaw rate, and lateral flapping angle. The control inputs are lateral and directional control in equivalent inches of stick and pedal position. The plant outputs are yaw and roll rate measured in deg/s. The state space model of the plant can be written as Eq. (2). This is a relatively simple third-order linear model. A number of dynamic states

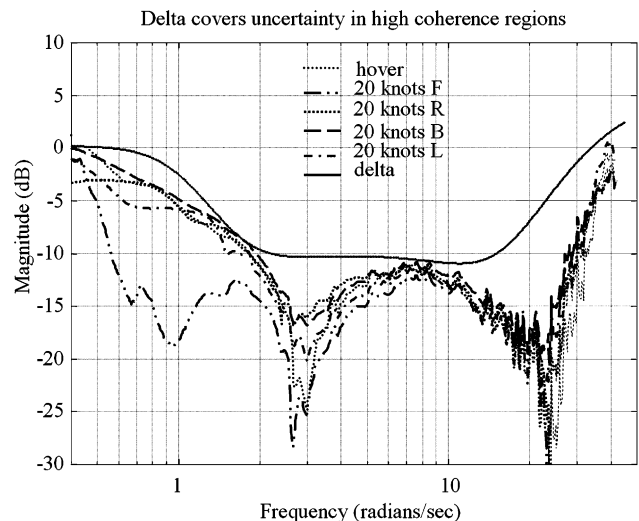


Fig. 3. Model uncertainty in the roll axis.

have been truncated. The complexity of the model could be increased by including lateral speed and roll attitude to better match the low-frequency dynamics. Flapping rate and lag dynamics could also be included to match the high-frequency dynamics. This would result in smaller uncertainty bounds, but a more complex plant model. The approach here is to use a simplified plant dynamic model and allow the uncertainty bounds in the robust control synthesis to account for the discrepancies.

$$\dot{\mathbf{x}} = \mathbf{A}\mathbf{x} + \mathbf{B}\mathbf{u},$$

$$\mathbf{y} = \mathbf{C}\mathbf{x},$$

$$\mathbf{x} = \begin{bmatrix} p \\ r \\ \beta_{1s} \end{bmatrix}, \quad \mathbf{u} = \begin{bmatrix} \delta_{lat} \\ \delta_{ped} \end{bmatrix}, \quad \mathbf{y} = \begin{bmatrix} p \text{ deg/s} \\ r \text{ deg/s} \end{bmatrix},$$

$$\mathbf{A} = \begin{bmatrix} 0 & 0.82 & 37.1 \\ -0.063 & -1.21 & 2.1 \\ -1.075 & 0 & -8.25 \end{bmatrix},$$

$$\mathbf{B} = \begin{bmatrix} 0.39 & -0.36 \\ 0 & 0.74 \\ 0.24 & 0 \end{bmatrix}, \quad \mathbf{C} = \begin{bmatrix} 57.3 & 0 & 0 \\ 0 & 57.3 & 0 \end{bmatrix}. \quad (2)$$

p = roll rate (rad/s)

r = yaw rate (rad/s)

β_{1s} = lateral flapping angle (rad)

δ_{lat} = lateral control (in)

δ_{ped} = directional control (in).

The augmented plant model includes additional dynamics due to the ideal response models, frequency weighted performance, and frequency weighted uncertainty bounds. Fig. 4 shows a schematic of the augmented plant model.

Output multiplicative uncertainty is used to account for the uncertainties that arise from model simplification and variation in operating point. The uncertainty

associated with the plant is represented by

$$\Delta(s) = \frac{G(s) - G_{nom}(s)}{G_{nom}(s)}. \quad (3)$$

The frequency variation of the uncertainty is calculated using Eq. (3), where $G(j\omega)$ is identified from the non-linear model and $G_{nom}(j\omega)$ is the frequency response of the simplified linear model. A weighting function must be designed that covers the model uncertainty over the entire low speed flight envelope. The following uncertainty weighting matrix was derived to cover the plant uncertainties.

$$\mathbf{W}_\Delta(s) = r_i \begin{bmatrix} \Delta_{11}(s) & 0 \\ 0 & \Delta_{22}(s) \end{bmatrix}, \quad (4)$$

$$\Delta_{11}(s) = \frac{13.157(s^2 + 0.9761s + 3.421)(s^2 + 4.554s + 59.54)}{(s^2 + 1.188s + 1.062)(s^2 + 36.35s + 2614)},$$

$$\Delta_{22}(s) = \frac{1.7891(s^2 + 1.873s + 3.065)(s^2 + 15.53s + 234.7)}{(s^2 + 1.248s + 1.011)(s^2 + 55.16s + 1251)},$$

where r_i is the radius of uncertainty used for the controller. When $r_i = 1$, the plant uncertainty is entirely covered by the weighting functions as shown in Fig. 3. The figure shows that the model is relatively accurate in the frequency range of 2–20 rad/s, but the model error approaches 100% for lower and higher frequencies. When r_i is selected to be less than unity, less conservative uncertainty bounds are used with the risk of instability.

The control design is based on an implicit model following approach. Ideal response characteristics for the yaw and roll axes are specified in the augmented plant in order to meet or exceed the handling qualities criteria for military rotorcraft (Aeronautical Design Standard, ADS-33E-PRF, 1999). The ideal response model provides a guideline in terms of relative system performance in terms of bandwidth, which is defined in the handling qualities specification as the frequency where the aircraft attitude lags the pilot input by -135° . This corresponds to the frequency where the phase angle of the angular rate response is -45° . Simple first-order transfer functions for the response of roll rate due to roll rate command and yaw rate due to yaw rate command are specified as

$$\mathbf{G}_{ideal}(s) = \begin{bmatrix} \frac{1}{0.1s + 1} & 0 \\ 0 & \frac{1}{0.2s + 1} \end{bmatrix}. \quad (5)$$

If the ideal response were tracked perfectly, then the bandwidth frequency is equal to the inverse of the time constant in the ideal response model. Thus, the

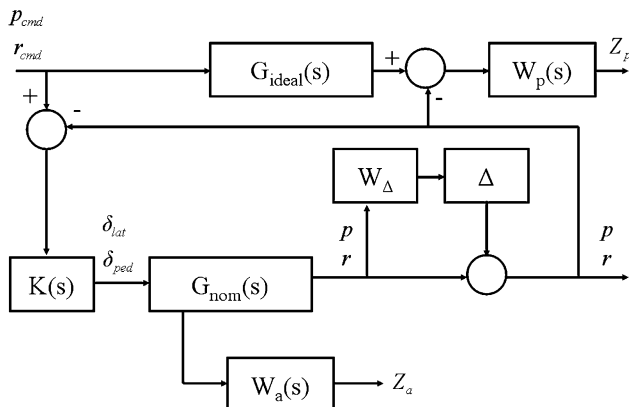


Fig. 4. Augmented plant model.

controller is designed to achieve a bandwidth of 10 and 5 rad/s in the roll and yaw axes, respectively. In this study, the objective is to significantly improve upon the agility of current rotorcraft, so these values are significantly larger than the bandwidth requirements currently specified for military rotorcraft (ADS-33E-PRF, 1999). In practice, perfect tracking is not achieved, so the actual bandwidth is expected to be lower than the value specified in the ideal response model. The degree to which the aircraft follows the ideal response model will be largely based on the relative weighting of tracking and actuator performance as well as the effective uncertainty bounds used in the probabilistic robust control design. The augmented plant includes frequency weighed performance for the tracking and actuator performance. The tracking performance weights are designed to emphasize low-frequency tracking and minimize steady-state error:

$$\mathbf{W}_p(s) = P_{weight} \begin{bmatrix} \frac{s+0.2}{s+0.01} & 0 \\ 0 & \frac{s+0.2}{s+0.01} \end{bmatrix}. \quad (6)$$

The actuator weights are designed to penalize high-frequency actuator activity and allow steady-state actuator motion:

$$\mathbf{W}_a(s) = 0.2 * P_{weight} \begin{bmatrix} \frac{s}{s+0.2} & 0 \\ 0 & \frac{s}{s+0.2} \end{bmatrix}. \quad (7)$$

The performance weighting parameter P_{weight} can be adjusted to achieve varying levels of performance. Increasing this performance weight, P_{weight} , and relaxing the radius of uncertainty, r_i , is expected to improve the tracking performance but allow greater risk of closed-loop instability.

Note that the simplified linear model discussed above is used for flight control design in the hover and low-speed flight regime. Similar models can be derived for forward flight conditions in order to design a suite of controllers for the entire flight envelope. Although the control design is based on simple linear models, the controllers are eventually tested on the full-order non-linear model discussed in Section 2.1.

5. Controller design procedure

If the full radius of uncertainty, $r_i = 1$, were used in Eq. (4), and the controller were designed to achieve a closed-loop structured singular value less than or equal to unity, then the system would have guaranteed closed-loop stability for all possible complex uncertainty perturbations. Such a controller could not be found for the plant model used in this study. The uncertainty

perturbations are too severe. When $r_i = 1$, even as the performance weighting parameter P_{weight} approaches zero, the structured singular value could not be made less than one, which theoretically implies that there is no controller that can robustly stabilize the plant. However, it is known that the robust control design is conservative, and in practice a controller synthesized with a reduced radius of uncertainty will result in a stable closed-loop system.

To design the risk-adjusted controller, a grid of the interval [0,1] was defined for the radius of uncertainty, r_i . For each of the points of the grid, the μ -toolbox of Matlab was used to design a controller that maximizes nominal performance while robustly stabilizing the closed-loop system subject to uncertainty of radius r_i . This was achieved by iteratively increasing the performance weight, P_{weight} , until the optimization resulted in a $\mu = 1$. The controllers obtained were of 25th order. Hankel-norm model reduction techniques were employed to lower the order of the controllers to 9. These controllers do not robustly stabilize the plant, so Monte-Carlo simulation was performed to determine the associated risk of instability for each controller. A set of random transfer functions were generated using the algorithm in Lagoa et al. (2001b) to model uncertainty perturbations (this process is discussed in the following section). A total of 10,000 samples were used to estimate the risk factor associated with each controller, where risk factor is defined as the percentage of cases where the theoretical uncertainty perturbation results in instability. Hence, a set of controllers with varying levels of risk are derived, as presented in Table 1. Each controller was also evaluated in terms of performance using the nominal plant model. The roll axis and yaw axis bandwidths were calculated according to handling qualities specifications (ADS-33E-PRF, 1999) and are shown in the table in units of rad/s.

The results in Table 1 show the expected trend in risk/performance tradeoff. ADS-33 defines the attitude bandwidth of an aircraft as the frequency where the attitude response lags the primary control input by 135°. A rotorcraft with high bandwidth flight controls will respond more quickly to pilot control inputs and will more readily track pilot commands at higher frequencies. As discussed in Section 4, the ideal response models were chosen to achieve a roll and yaw bandwidth of 10 and 5 rad/s, respectively. These values are substantially higher than those required for Level I handling qualities in ADS-33. However, future rotorcraft missions may require more agile rotorcraft, which would require higher bandwidth flight controls. Thus bandwidth is a suitable measure of performance. The bandwidths for the high-risk controllers are relatively high, and nearly achieve the bandwidth specified in the ideal response model, but the risk analysis indicates those controllers also have a higher risk of inducing

Table 1
Risk and performance of controllers

Controller	r_i	P_{weight}	Risk factor	Roll BW	Yaw BW
C1	0.001	2.52	0.4552	8.8	4.5
C2	0.010	2.00	0.4178	8.8	4.5
C3	0.020	1.50	0.3949	8.8	4.5
C4	0.040	1.00	0.2889	8.0	4.3
C5	0.070	0.80	0.1876	7.5	4.1
C6	0.100	0.70	0.1555	7.0	4.0
C7	0.200	0.50	0.1353	6.2	3.6
C8	0.600	0.32	0.1176	5.1	3.0
C9	0.700	0.30	0.0841	3.1	2.6

closed-loop instability. For the low-risk controllers, the bandwidth is substantially degraded, but those controllers have a much lower risk of initiating instability.

As discussed in the following section, the measure of risk is determined by generating a large sample of perturbations uniformly distributed over the entire space of possible uncertainties as defined by the weighting functions in Eq. (4). A risk factor of X% does not mean that there is an X% chance that the aircraft will become unstable, only that X% of the theoretical uncertainty perturbations result in instability. In practice, the probability of the uncertainty perturbations is not uniformly distributed. Perturbations within some portions of the space of uncertainty are more or less likely to occur than others. Although the risk factor in Table 1 gives some measure of risk relative to the other controllers, it does not explicitly define the probability of instability for a given controller. For example, controller 9 was found to have a risk factor of 8%, but in extensive simulation testing with the full non-linear model it never resulted in instability.

6. Sample generation procedure

To address the problem of risk assessment in the presence of dynamic uncertainty, recent results on probabilistic robustness were applied. The algorithm in Lagoa et al. (2001b) was used to generate a set of random transfer functions to represent the uncertainty perturbations, $\Delta(s)$. The algorithm generates random discrete-time transfer functions in the set:

$$F_n = \left\{ \begin{array}{l} H(z) = h_0 + h_1 z + \dots + h_{n-1} z^{n-1} : \\ \|H(z) + z^n G(z)\|_\infty \leq 1 \text{ for some stable } G(z) \end{array} \right\} \quad (8)$$

This is a set of random transfer functions in the discrete-time domain, which can be completed to a transfer function with infinity norm ≤ 1 . The random transfer functions are then transformed to the continuous-time

domain using Tustin transformations. The algorithm is described below.

Step 1: Let $k = 0$. Generate N^* samples of h_0 uniformly distributed over the interval $[-1, 1]$.

Step 2: Let $k = k + 1$. For every generated sample $\{h_0^l, h_1^l, \dots, h_{k-1}^l\}$, generate $N^*(M_k^l - m_k^l)$ samples of h_k uniformly over the interval $[M_k^l, m_k^l]$, where

$$m_k^l = -Y(H^l)^T Y^T - |1 - YY^T|,$$

$$M_k^l = -Y(H^l)^T Y^T + |1 - YY^T|,$$

$$H^l = \tilde{H}(0, h_0^l, \dots, h_{k-2}^l), \quad (9)$$

$$Y = [h_{k-1}^l \dots h_1^l \ h_0^l](I - (H^l)^T H^l)^{-1/2},$$

$$\tilde{H}(h_0, h_1, \dots, h_k) = \begin{bmatrix} h_k & \dots & h_1 & h_0 \\ h_{k-1} & \dots & h_0 & 0 \\ \vdots & & & \vdots \\ h_0 & 0 & \dots & 0 \end{bmatrix}.$$

Step 3: If $k = n - 1$, stop. Else go to Step 2.

7. Practical implementation issues

The controllers discussed above provide a roll rate command and yaw rate command response for the hover and low-speed flight regime. This is just one step required for practical implementation of a lateral-directional controller on an aircraft. The controller needs to be extended to operate in forward flight conditions and it needs to incorporate more advanced autopilot modes such as attitude hold, turn coordination, and heading hold. The issue of control switching must also be addressed.

The operating range of the controller has been extended into forward flight up to 140 knots (72.044 m/s). The same design procedure is repeated for forward flight conditions at 40 knots (20.584 m/s), 80

knots (41.168 m/s), and 120 knots (61.752 m/s): (1) identify the linear dynamics at nominal flight condition, (2) identify the dynamics at off-design conditions, (3) define the uncertainty weights that cover the multiplicative uncertainty, (4) define a suite of controllers with varying risk and performance. The uncertainty weights are based on frequency response data obtained at airspeeds ± 20 knots off of the nominal operating point.

The probabilistic robust controllers discussed above only provide inner-loop stabilization and results in a rate command response type. Outer-loop controllers can then be used to achieve autopilot functions such as roll attitude hold, heading hold, and turn coordination. Once the inner loop is closed, the lateral-directional dynamics of the aircraft behave as a pair of decoupled first-order systems, as dictated by the ideal response model. Thus, simple classical control theory can be used to design proportional or proportional plus integral compensators for the outer loop. Fig. 5 shows a schematic of an outer-loop controller that can be used to achieve for roll attitude command/attitude hold response in the roll axis and turn coordination in the yaw axis. If a proportional gain, K , is used in the roll attitude compensator, then the effective closed-loop transfer function for roll attitude response becomes

$$\frac{\phi}{\phi_{cmd}}(s) = \frac{K}{\tau s^2 + s + K}, \quad (10)$$

where τ is the time constant in the roll rate response as dictated by the ideal response model in Eq. (5). The gain K can be chosen to achieve the desired second-order dynamics in attitude response. For turn coordination, the control law derived in Rysdyk and Calise (1998) is used to regulate lateral acceleration, a_y .

$$r_{cmd} = (a_y \text{ cmd} - a_y + w p + g \sin \phi \cos \theta)/u, \quad (11)$$

where u, w, p, ϕ , and θ represent the longitudinal velocity, vertical velocity, roll rate, roll attitude, and pitch attitude of the aircraft, respectively.

Another topic that must be addressed is the issue of switching between controllers. As discussed in Section 5, the controller architecture results in a bank of controllers with different risk and performance levels.

Furthermore, as discussed above, several banks of controllers are designed for different airspeeds. The system will switch between controllers as the aircraft transitions to different airspeeds or when the upper-tier supervisor determines that it should switch to a higher or lower risk controller. The issue of instability due to switching between the controllers has to be addressed. A switching law is proposed which guarantees stability of the closed-loop system while the controllers are being switched.

It is shown in Morse (1996) that when all subsystems are Hurwitz stable, then the entire system is exponentially stable for any switching signal if the time between two consecutive switching operations, called the “dwell time”, is sufficiently large. Hespanha and Morse (1999) extend the concept of “dwell time” to “average dwell time”, which means the average time interval between two consecutive switching operations is no less than a specified constant. It was shown that if the average dwell time is sufficiently large, then the switched system is exponentially stable. The dwell time concept is a reasonable approach for real-time implementation since it is counter-intuitive and counter-productive to switch controllers too frequently.

For this system, an average dwell time is selected that is sufficiently large to guarantee the stability when switching between any of the controllers. A dwell time of 2 s was found to be sufficient for this application (this value was found experimentally and was not derived from rigorous analysis). When the decision is made to switch controllers, the current controller and the new controller are run simultaneously. The control signal is gradually switched between the two controllers over the 2 s dwell time. A “blend parameter” is ramped in over the 2 s interval and used to generate a weighted average of the two control signals. This approach was found to be sufficient to demonstrate the concepts in this paper, and a more rigorous approach to switching is left to future work.

8. Simulation results and discussion

This section presents and discusses the pertinent results of simulation experiments conducted on the rotorcraft control system discussed above. In this analysis, only the inner-loop controllers for hover/low-speed flight are considered. The forward flight controllers and the outer-loop control laws discussed in Section 7 are not presented here.

The controllers were implemented on the non-linear GENHEL simulation model. The very high-risk controllers (C1 and C2) were found to exhibit instability in almost all cases and thus were eliminated from the family of robust controllers. The controllers with medium-to-high risk tended to perform well, but they

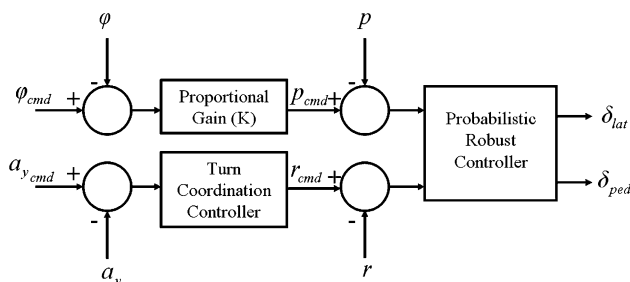


Fig. 5. Outer-loop control.

occasionally exhibited instability as the operating conditions were varied or for sufficiently large disturbances. The low-risk controllers resulted in significantly degraded performance but these controllers never resulted in instability in the non-linear simulation.

The most common form of instability resulted in sustained high-frequency oscillations when the lag progressing mode of the rotor became unstable. While this type of instability could be very dangerous and uncomfortable to the pilot, it also would be easily identifiable to a supervisory controller since the oscillations tend to have a unique frequency range. In some cases, it was observed that instability could occur due to a real pole passing the origin, which resulted in a very slow divergent mode. Such instability could be considered less dangerous on piloted aircraft, because pilots can easily compensate for it. However, this might be more problematic if the method is applied to unmanned vehicles since it would take longer for the supervisor to detect it. This type of instability can be eliminated using the outer-loop control laws discussed in Section 7. In this analysis, the detection of the instability is assumed once the high-frequency oscillations are observed. Formal treatment of the detection of instability by a supervisory controller has been addressed in detail in Tolani, Horn, Ray, and Chen (2004).

Two sets of time history results are presented in this paper. The time history shows the response to a doublet in roll rate command. A roll rate command of 10 deg/s to the right is held for 4 s and followed by a roll rate command of 10 deg/s to the left for 4 s. The figures show the response of roll rate and the lateral control input. Fig. 6 shows the response of the aircraft using a relatively high-risk controller C3. For moderately large inputs, the controller was found to cause limit cycle instability due to destabilization of the lag progressing mode. This can be observed in the high-frequency oscillation following the initial command. Fig. 7 starts

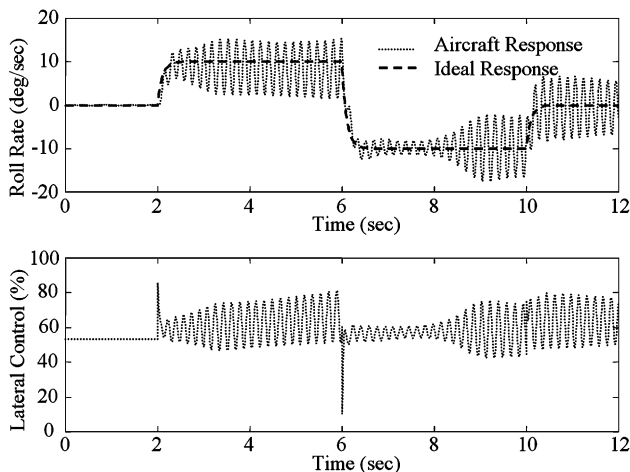


Fig. 6. Time history results for high-risk controller.

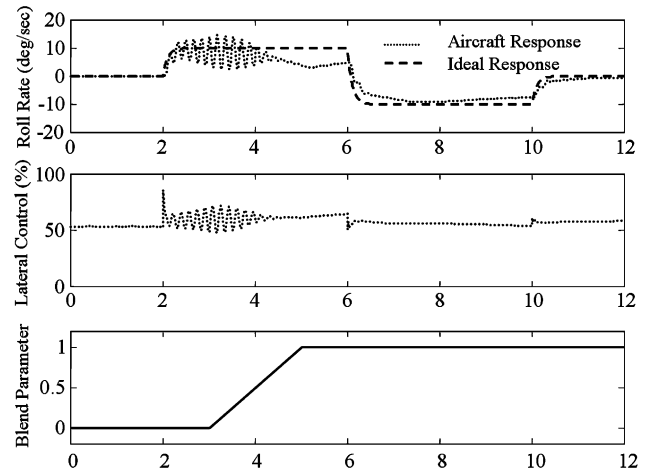


Fig. 7. Recovery from instability.

with the same high-risk controller but as soon as instability is detected a lower risk controller C7 is phased in between 3 and 5 s. State space representations of controllers C3 and C7 are run simultaneously, and the output the controller is a weighted average based on the blending parameter. By switching to the low-risk controller the instability is terminated. After which, the controller follows the command response in roll rate with a reasonable level of tracking performance.

9. Conclusions and future research

This paper presents a two-tier hierarchical architecture for future-generation rotorcraft control systems in order to achieve enhanced performance and reliability. The concept is validated using a non-linear simulation model. A bank of μ -controllers is designed where the robust stability requirements are relaxed with a specified probability in order to achieve better performance. Extensive Monte-Carlo simulations were conducted to demonstrate the expected trend in the risk level and performance as the weights were varied. The controller was demonstrated for the inner-loop stabilization of the lateral-directional dynamics of a helicopter in hover/low-speed flight. The approach for extending the controller to operate over the entire flight envelope and to provide outer-loop autopilot functions was also discussed.

It was observed that no controllers could be found that robustly stabilize the plant given the relatively large uncertainty bounds associated with the simple linear model used in the control synthesis. However, it was observed that controllers designed with relaxed uncertainty bounds resulted in consistently stable closed-loop dynamics over a range of operating conditions when tested with the high order, non-linear simulation. Clearly, a design approach with strict robust stability

requirements results in excessive conservatism. Such an approach would only be feasible if a significantly enhanced plant model with less uncertainty were used, which would in turn increase the complexity of both the system identification process and the controller. Therefore, the use of a probabilistic robust design method is of interest for complex and uncertain dynamic systems such as rotorcraft. The benefits of such an approach can be enhanced by allowing the system to increase the risk of instability to achieve better performance, as long as a method is in place to recover upon the onset of instability. The available performance of the flight controller can then effectively be maximized for any given flight condition. The idea of allowing a small well-defined risk of instability for enhanced performance works only because there is an upper-tier supervisory controller that detects instability and mitigates it by switching to a more conservative controller. This approach could potentially be used for other non-linear complex dynamical systems that operate over a wide range of conditions.

Current work has focused on extending the operating regime out to 140 knots (72.044 m/s) forward speed and developing a more rigorous approach to control switching. For future research, the probabilistic robust controller will be augmented with an upper-tier discrete-event supervisor for reliable operation over a wide range. This augmented supervisory control system will autonomously determine the desired level of performance based on environmental and operational conditions. The integrated control system would have the capability for early detection of instabilities based on the available sensor data and additional information on vehicle operation and maintenance. This work has been partially completed and the issues of early detection of stability are addressed in Tolani et al. (2004).

References

- Aeronautical Design Standard-33E-PRF. (1999). *Handling qualities requirements for military rotorcraft*. St. Louis, MO: U.S. Army Aviation Systems Command; 1999.
- Dryfoos, J. B., Kothmann, B. D., & Mayo, J. (1999). An approach to reducing rotor-body coupled-roll oscillations on the RAH-66 comanche using modified roll rate feedback. *55th Annual forum of the American Helicopter Society*. Montreal, Canada, June 1999.
- Hespanha, J. P., & Morse, A. S. (1999). Stability of switched systems with average dwell-time. *Proceedings of 38th IEEE conference on decision and control*. pp. 2655–2660.
- Horn, J. (2002). Rotor state feedback for high bandwidth control and structural load limiting. *American Helicopter Society flight controls and crew systems technical specialists meeting*. Philadelphia, PA, October 2002.
- Howlett, J. (1989). *UH-60A BLACK HAWK engineering simulation program: volume I—mathematical model*. NASA CR-177542, USAAVSCOM TR 89-A-001, September 1989.
- Ingle, S. J., & Celi, R. (1992). Effects of higher order dynamics on helicopter flight control law design. *48th Annual forum of the American Helicopter Society*. Washington, DC, June 1992.
- Lagoa, C. M. (1999). A convex parameterization of risk-adjusted stabilizing controllers. *Proceedings of the 38th IEEE conference on decision and control*. Phoenix, AZ, December 1999.
- Lagoa, C. M., Li, X., & Sznaier, M. (2001a). Application of probabilistically constrained linear programs to risk-adjusted controller design. *Proceedings of the 2001 American control conference*. Arlington, VA, June 2001.
- Lagoa, C. M., Sznaier, M., & Barmish, B. R. (2001b). An algorithm for generating transfer functions uniformly distributed over H-infinity balls. *Proceedings of the 40th IEEE CDC*. Orlando, Florida, December 2001.
- Morse, A. S. (1996). Supervisory control of families of linear set-point controllers—part 1: exact matching. *IEEE Transactions on Automatic Control*, 41(10), 1413–1431.
- Rysdyk, R. T., & Calise, A. J. (1998). Adaptive model inversion flight control for tiltrotor aircraft. *American Helicopter Society 54th annual forum*. Washington, DC, May 1998.
- Sahasrabudhe, V., & Celi, R. (1997). Improvement of off-design characteristics in integrated rotor-flight control system optimization. *AHS, annual forum 53rd Virginia Beach, VA, April 29–May 1, 1997, Proceedings*. Alexandria, VA, American Helicopter Society, 1997. Vol. 1 (A97-29180 07-01).
- Smerlas, A., Postlethwaite, I., Walker, D. J., Strange, M. E., Howitt, J., Horton, R. I., Gubbels, A. W., & Baillie, S. W. (1998). Design and flight testing of an H-infinity controller for the NRC Bell 205 experimental fly-by-wire helicopter. *AIAA GNC conference*, Boston, MA, 1998.
- Takahashi, M. (1994). Rotor-state feedback in the design of flight control laws for a hovering helicopter. *Journal of the American Helicopter Society*, 39(1), 50–61.
- Tischler, M. B. (1991). System identification requirements for high-bandwidth rotorcraft flight control system design. *American control conference*, Boston, MA, June 1991.
- Tolani, D. K., Horn, J. F., Ray, A., & Chen, J. (2004). Hierarchical control of future generation rotorcraft. *American control conference*. Boston, USA. June 29th–July 2nd 2004.